

The W.R. Wiley Environmental Molecular Sciences Laboratory (EMSL) is a U.S. Department of Energy (DOE) national scientific user facility located at Pacific Northwest National Laboratory (PNNL) in Richland, Washington. EMSL is operated by PNNL for the DOE Office of Biological and Environmental Research. At one location, EMSL offers a comprehensive array of leading-edge resources in six research facilities.

Access to the capabilities and instrumentation in EMSL facilities is obtained on a peer-reviewed proposal basis, and users are participants on accepted proposals. EMSL staff members work with users to expedite access to the facilities and the resident scientific expertise. The bimonthly report documents research and activities of EMSL staff and users.

## Research Highlights

### Quantification of Actinide [Alpha]-Radiation Damage in Minerals and Ceramics

I Farnan,<sup>(a)</sup> HM Cho,<sup>(b)</sup> and WJ Weber<sup>(b)</sup>

(a) *University of Cambridge, Cambridge, United Kingdom*

(b) *Pacific Northwest National Laboratory, Richland, Washington*

*By using solid state nuclear magnetic resonance (NMR), we demonstrated that structural damage in plutonium (Pu)-doped zircon could be directly quantified. This finding is important to estimate the resistance to self-irradiation damage of materials incorporating actinides for long-term immobilization (i.e., over thousands of years).*

One significant problem facing the world is safe disposal of unneeded, long-lived radioisotopes. It has been proposed to incorporate radioisotopes of elements, such as plutonium, americium, and curium, in a fixed, durable matrix until their radiation levels naturally decay to safe levels. While glass is favored by many scientists, crystalline solids such as zircon ( $ZrSiO_4$ ) are also under consideration. However, prolonged exposure to the alpha-emissions of the encapsulated

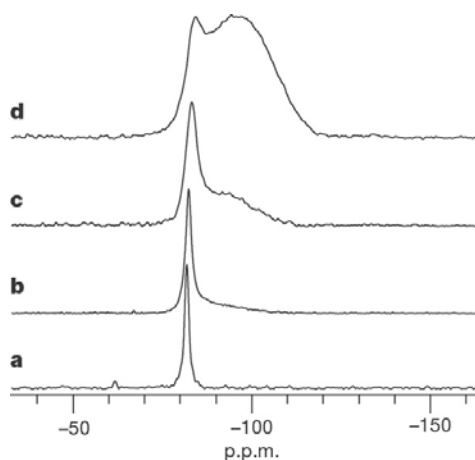


**Figure 2.**  $^{29}\text{Si}$  NMR spectrum of zircon after accumulating the following doses of alpha particles. (a) no  $\alpha$  decay, (b)  $1.2 \times 10^{18}$   $\alpha/\gamma$ , (c)  $2.9 \times 10^{18}$   $\alpha/\gamma$ , (d)  $7.1 \times 10^{18}$   $\alpha/\gamma$ .

radioisotopes can cause crystalline structures to become amorphous over time. The relatively heavy and energetic alpha particle

will break bonds and move atoms, and the main heavy atom recoils with a slower velocity, but equal energy, and also is able to disrupt the crystal structure (Figure 1). The result is a cumulative disruption of the crystal arrangement.

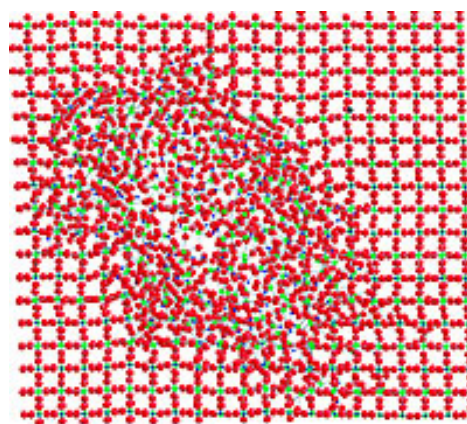


**Figure 1.** Results of a calculation showing the disruption to a zircon crystal lattice caused by alpha particle emission from the decay of a single plutonium atom.

Because zircon contains silicon,  $^{29}\text{Si}$  NMR can be used to monitor the nature of the silicon sites in the zircon crystal. Initially, all of the sites will be identical and will give a single sharp line in the NMR spectrum. As the crystal is disrupted,

the peak of atoms from damaged sites shifts and broadens, reflecting the disorganized state of the silicon at these sites. By comparing the area of the sharp peak and the broad peak, it is possible to estimate the extent of disruption of the crystal structure caused by exposure to alpha irradiation from the incorporation of plutonium (Figure 2).

Looking at samples with different levels of plutonium incorporation that have been aged for a number of years will give an estimate of the amount of damage that has accumulated over the time period. Based on this study, zircons with 10 wt.% plutonium incorporation will start to swell in 210 years and be completely amorphous in 1400 years. The time scale of this process compares unfavorably with the half-life of  $^{239}\text{Pu}$ , which is 24,100 years.

#### Citation

Farnan I, HM Cho, WJ Weber, 2007. “Quantification of Actinide  $\alpha$ -Radiation Damage in Minerals and Ceramics.” *Nature* 445(7124):190-193.

## Particokinetics *In Vitro*: Dosimetry Considerations for *In Vitro* Nanoparticle Toxicity

JG Teeguarden,<sup>(a)</sup> PM Hinderliter,<sup>(a)</sup> G Orr,<sup>(a)</sup> BD Thrall,<sup>(a)</sup> and JG Pounds<sup>(a)</sup>  
(a) *Pacific Northwest National Laboratory, Richland, Washington*

*The purpose of this work is to improve the basis for in vitro assessment of nanoparticle toxicity by advancing the understanding of particle solution dynamics in cell culture media as they relate to dosimetry and dose-response assessment. These results begin to address the urgent need for rapid hazard assessment of emerging nanoparticles through development of suitable high-throughput in vitro assays.*

Developing testing strategies that can meet the burgeoning demand to characterize the hazard potential of the considerable number of nanomaterials that have been or will be produced is one of the most significant challenges faced by the regulatory, research, and producer communities. *In vitro* studies, which have become an essential component of risk assessment-directed research paradigms for chemicals, pharmaceuticals, consumer products, and fine and ultrafine particulates, are an essential element of all tiered approaches for toxicity assessment of nanomaterials that have been proposed.

Despite the considerable attention that *in vitro* systems have received and their growing application to nanomaterial toxicity assessment, little attention has been devoted to a critical examination of their suitability, particularly when it comes to particle solution dynamics and dosimetry. In contrast to soluble chemicals, nanoparticles can settle, diffuse, and aggregate differentially according to their size, density, and surface physicochemistry. These processes are expected to significantly affect the cellular dose. The definition of dose for nanoparticles in an *in vitro* system is, therefore, more dynamic, more complicated, and less comparable across particle types than it is for soluble chemicals. Before adequate dose-response assessments for nanomaterials can be conducted, there is a need to develop a better understanding of these processes, how particle and media characteristics affect them, and their potential impact on cellular dose *in vitro*.

The purpose of this research is to improve the basis for *in vitro* assessment of nanoparticle toxicity by advancing the understanding of particle solution dynamics in cell culture media as they relate to dosimetry and dose-response assessment. Particles in general and nanoparticles specifically, diffuse, settle, and agglomerate in cell culture media as a function of systemic and particle properties: for example, media density and viscosity, and particle size, shape, charge, and density. Cellular dose then is also a function of these factors as they determine the transport rate of nanoparticles to cells in culture.

Dose amount and time (i.e., both the time of dose and the duration of dose) are two key elements that must be considered for *in vitro* chemical dosimetry. Dose for nanoparticles *in vitro* can be defined at various levels of specificity with regard to the site and mode of action: administered dose is the most nonspecific level, while apparent exposure is a more specific level, and cellular dose is the most specific level. This concept is illustrated in Figure 1, which shows time-resolved images of an alveolar epithelial cell (C10) grown in culture and exposed to fluorescence-tagged, 500-nm amorphous silica particles. The three panels show the uptake of the nanoparticles in time. Panel 1 illustrates delivered dose, a silica particle (the green at the tip of the arrow) on the apical surface of the cell. In time, the particle is no longer visible as the focal plane moves into the interior of the cell (Panel 2). In Panel 3, the silica particle has been taken up into the cell and is observed as the focal plane moves farther into the interior of the cell.

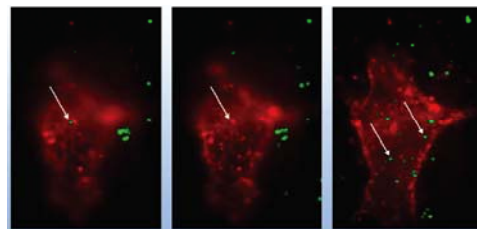


**Figure 1.** Images of an alveolar epithelial cell (C10), grown in culture and exposed to fluorescence-tagged 500-nm amorphous silica particles. The three panels show the uptake of the nanoparticles in time.

As illustrated in Figure 1, the delivered dose also has the advantage of being directly scaleable and comparable to metrics of dose commonly used for particulates *in vivo*; for example, the delivered dose per surface area of cells in culture can be compared with the dose delivered/surface area of respiratory tract tissues. Intracellular sites of action such as the endosome, lysosome, or phagolysosome are best represented by more specific metrics of dose such as internalized mass, surface area, or number of particles or their amounts in specific intracellular compartments. These dose metrics have the advantage of accounting for size or other particle-dependent differences in cellular uptake and can also be tailored to a mode of action, although in practice, they are difficult to measure.

In this research, we develop and apply the principles of dosimetry *in vitro* and outline an approach for simulating nanoparticle particokinetics in cell culture systems. We also illustrate that where equal mass concentrations (mg/ml) imply equal doses for dissimilar materials, the corresponding particle number or surface area concentration doses differ by orders of magnitude. More importantly, when rates of diffusional and gravitational particle delivery are accounted for, trends and magnitude of the cellular dose as a function of particle size and density differ significantly from those implied by “concentration” doses. For example, 15-nm silver nanoparticles appear ~4000 times more potent than micron-sized cadmium oxide particles on a  $\text{cm}^2/\text{ml}$  media basis, but are only ~50 times more potent when differences in delivery to adherent cells are considered.

Often, simple surrogates of dose can cause significant misinterpretation of response and uptake data for nanoparticles *in vitro*. Incorporating particokinetics and principles of dosimetry would significantly improve the basis for nanoparticle toxicity assessment, thus increasing the predictive power and scalability of such assays. This work was featured on the cover of the February 2, 2007, issue of *Toxicological Sciences* (Figure 2).

#### Citation

Teeguarden JG, PM Hinderliter, G Orr, BD Thrall, and JG Pounds. 2007. “Particokinetics *In Vitro*: Dosimetry Consideration for *In Vitro* Nanoparticle Toxicity Assessments.” *Toxicological Sciences* 95(2):300-312.

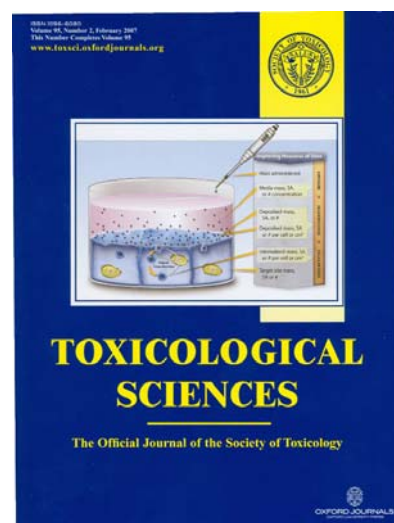


**Figure 2.** Cover of the February 2, 2007, issue of *Toxicological Sciences*.

## Correlation between Fundamental Binding Forces and Clinical Prognosis of *Staphylococcus aureus* Infections of Medical Implants

R Yongsunthona,<sup>(a)</sup> VG Fowlere, Jr.,<sup>(b)</sup> BH Lower,<sup>(c)</sup> FP Vellano III,<sup>(a)</sup> E Alexander,<sup>(b)</sup> LB Reller,<sup>(b)</sup> GR Corey,<sup>(b)</sup> and SK Lower<sup>(a)</sup>

(a) *Ohio State University, Columbus, Ohio*

(b) *Duke University, Durham, North Carolina*

(c) *W.R. Wiley Environmental Molecular Sciences Laboratory, Richland, Washington*

*In this study, we used atomic force microscopy to show that pathogenic strains of Staphylococcus aureus are able to attach to substrates simulating an implant device much more efficiently than nonpathogenic control strains of S. aureus. These results suggest that pathogenic strains express specific surface-exposed proteins that allow the bacteria to bind to the surface of an implant. They also suggest that one way to prevent S. aureus-related device infections is to prohibit the initial binding reaction itself.*

In the United States, surgical implants (e.g., prosthetic heart valves or pacemakers) significantly improve the quality of life for many people but, paradoxically, place these same patients at risk for life-threatening infections. These infections are frequently caused by pathogenic strains of *S. aureus* that adhere to the surface of the implant allowing the bacteria to form a biofilm that is difficult to combat with host defenses or antibiotics. SK Lower of Ohio State University and co-workers from Duke University Medical Center and EMSL had a manuscript accepted by the American Chemical Society journal *Langmuir* in January 2007. This article describes the work that Lower conducted in collaboration with BH Lower (EMSL) as part of their EMSL Science Theme Project, Substrate-Specific Binding of Staphylococcus Adhesins to Solid Surfaces. This project is managed by NJ Hess (EMSL) and also includes collaborations with Dr. VG Fowler's group from Duke University Medical Center. The title of their article is "Correlation between Fundamental Binding Forces and Clinical Prognosis of *Staphylococcus aureus* Infections of Medical Implants" and their results suggest that *S. aureus*' "force taxonomy" may provide a fundamental and practical indicator of the pathogen-related risk that infections pose to patients with implanted medical devices (Figure 1). The note can viewed early in published form at [http://pubs3.acs.org/acs/journals/doi/lookup?in\\_doi=10.1021/la063117v](http://pubs3.acs.org/acs/journals/doi/lookup?in_doi=10.1021/la063117v).

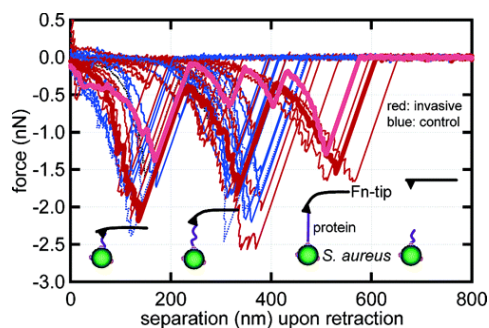


**Figure 1.** Retraction force profiles (i.e., force spectra) collected as an Fn-coated probe was pulled from contact with the cell wall of *S. aureus*. Shown are randomly selected curves from the eight control isolates (blue) and seven invasive isolates (red). The lighter red curve was collected on a mutant strain of *S. aureus* that overproduces FnBP on its cell wall. The phenotype of this mutant strain is described in Greene et al. (1995).

### Citation

Greene C, D McDevitt, P Francois, PE Vaudaux, DP Lew, and TJ Foster. 1995. "Adhesion Properties of Mutants of *Staphylococcus aureus* Defective in Fibronectin-binding Proteins and Studies on the Expression of fnb Genes." *Molecular Microbiology* 17(6):1143-1152.

Yongsunthon R, VG Fowler, Jr., BH Lower, FP Vellano III, E Alexander, LB Reller, GR Corey, and SK Lower. 2007. "Correlation between Fundamental Binding Forces and Clinical Prognosis of *Staphylococcus aureus* Infections of Medical Implants." *Langmuir* ASAP Web Release Date: 03-Feb-2007; (Letter) DOI: 10.1021/la063117v.

## Comparing Proteomics Analysis of Nipple Aspirate Fluids: Discovering Biomarkers for Early Detection of Breast Cancer

T Liu,<sup>(a)</sup> MA Gritsenko,<sup>(a)</sup> DG Camp,<sup>(a)</sup> F Esteva,<sup>(b)</sup> L Hartwell,<sup>(c)</sup> and RD Smith<sup>(a)</sup>

(a) Pacific Northwest National Laboratory, Richland, Washington

(b) University of Texas M.D. Anderson Cancer Center, Houston, Texas

(c) Fred Hutchinson Cancer Research Center, Seattle, Washington

*This study represents the largest scale characterization of the nipple aspirate fluid proteome to date. The in-depth comparison of nipple aspirate fluid from cancerous and contralateral non-cancerous breasts of women with early-stage breast cancer provides a basis for early detection of breast cancer.*

Breast cancer is the most common type of cancer and the second leading cause of cancer deaths in women in the United States. Presymptomatic screening to detect early-stage breast cancer could potentially reduce breast cancer-related mortality. Unfortunately, currently available breast cancer screening tools such as mammography and breast examination miss up to 40 percent of early-stage breast cancers. In addition, an invasive biopsy (e.g., needle or surgical biopsy) must typically be performed to confirm the presence of malignant disease by cytologic or histologic evaluation, if an area of suspicion is identified by the screening. Therefore, it is of crucial importance to develop noninvasive techniques that would complement current methodologies for the detection and prognosis of small breast lesions at the molecular level, providing a significant opportunity to distinguish between malignant and benign lesions and to treat a neoplasm before it invades the tissue.

The breast epithelium exfoliates cells as a renewal of tissue and secretes fluids into its ductal and lobular system, where most breast carcinomas (approximately 70 to 80 percent) originate. Using a handheld suction cup, this breast fluid can be extracted noninvasively through the nipple and is thus referred to as nipple aspirate fluid (NAF). Compared with serum/plasma, proximal fluids from the breast potentially offer a superior source of biomarkers for breast cancer because the proteins present are specifically released from breast tumor tissue. Several studies have indicated that NAF contains potentially diagnostic or prognostic markers of breast cancer and, in particular, the application of proteomics for developing more specific biomarkers appears to be promising (Varnum et al. 2003; Alexander et al. 2004; Pawlik et al. 2006). However, these studies provided only very limited NAF protein identifications (<100), presumably because of the low protein yields and the high dynamic range of protein abundances in the breast fluid.

In this study, NAF samples from 15 early-stage breast cancer patients were used to generate a pooled sample using NAF from the diseased breast and a non-cancerous pool using NAF from the contralateral disease-free breast. The overall comparative proteomics strategy is depicted in Figure 1. To improve the detection in downstream proteomics analysis, 12 proteins of high abundance were initially removed from both the cancerous and non-cancerous NAF pools separately by applying an IgY-12 immunoaffinity depletion chromatography step. Both the flow-through (i.e., lower abundance proteins) and the bound (i.e., the 12 high-abundance proteins and potentially other proteins that bind through mechanisms such as protein-protein interaction) portions were subjected to trypsin digestion. Next, the resulting tryptic peptides were separated into cysteinyl peptides and non-cysteinyl peptides through the cysteinyl peptide enrichment (CPE) procedure, followed by strong cation exchange chromatography (SCX) fractionation and LC-MS/MS analyses.

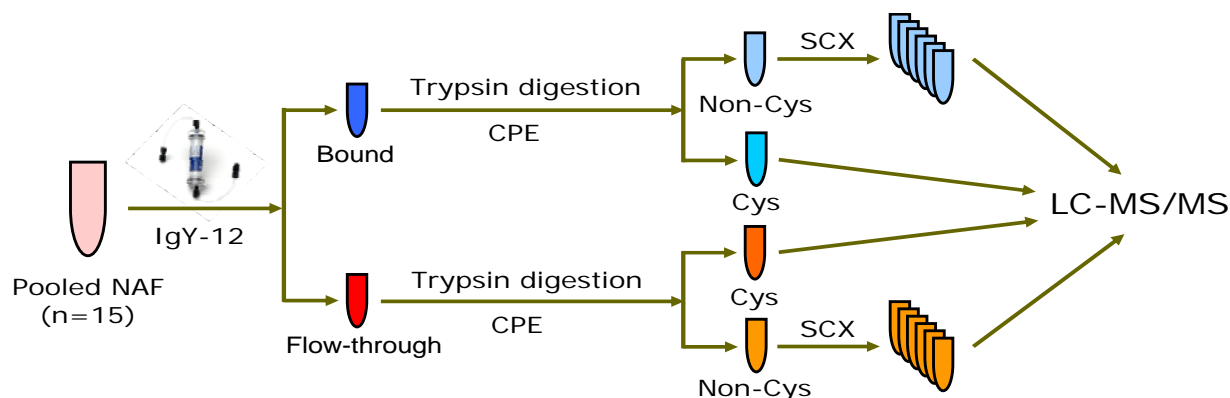


**Figure 1.** Schematic illustration of large-scale analysis of NAF by liquid chromatography-tandem mass spectroscopy (LC-MS/MS).

The highly effective combination of immunoaffinity depletion, in-depth fractionation, and ultrahigh resolution LC separation employed in this study led to the confident identification of a total of 11,364 unique peptides and 1997 non-redundant proteins, representing the most comprehensive proteome coverage to date for human NAF. Significantly, comparative analysis of the IgY-12 flow-through proteins using spectrum counting revealed 470 proteins expressed solely in the cancerous NAF, exemplified by ErbB-3, which has been previously found over-expressed in breast carcinomas using real-time quantitative RT-PCR assays. A group of 220 proteins displayed greater than a threefold increase in abundance in the cancerous NAF (Figure 2). Many over-expressed proteins detected in this investigation are known to be correlated to breast carcinomas from previous studies that measured either their mRNA levels using microarray or protein levels using ELISA. It is anticipated that NAF proximal fluid analysis in conjunction with the proteomic analysis of other breast tissue-derived samples (e.g., tumor interstitial fluid, ductal lavage fluid) that additional specific and sensitive breast cancer biomarkers can be discovered. The subsequent pre-clinical validation of these candidate biomarkers through the application of affinity reagents in combination with either multi-protein biomarker panels or multiple reaction monitoring (MRM) experiments would thereby advance the goal of early detection of breast cancer through a blood test.

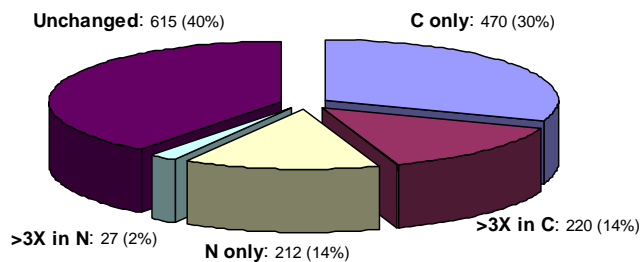


**Figure 2.** Differential expression of NAF proteins. N = normal contra-lateral NAF; C = cancerous NAF.

## Citations

Alexander H, AL Stegner, C Wagner-Mann, GC Du Bois, S Alexander, and ER Sauter. 2004. "Proteomic Analysis to Identify Breast Cancer Biomarkers in Nipple Aspirate Fluid." *Clinical Cancer Research* 10(22):7500-7510.

Pawlik TM, DH Hawke, Y Liu, S Krishnamurthy, H Fritsche, KK Hunt, and HM Kuerer. 2006. "Proteomic Analysis Of Nipple Aspirate Fluid from Women with Early-Stage Breast Cancer Using Isotope-Coded Affinity Tags and Tandem Mass Spectrometry Reveals Differential Expression of Vitamin D Binding Protein." *BMC Cancer* 66(68):8-77.

Varnum SM, CC Covington, RL Woodbury, K Petritis, LJ Kangas, MS Abdullah, JG Pounds, RD Smith, and RC Zangar. 2003. "Proteomic Characterization of Nipple Aspirate Fluid: Identification of Potential Biomarkers of Breast Cancer." *Breast Cancer Research and Treatment* 80(1):87-97.

## Irradiation Behavior of SrTiO<sub>3</sub> at Temperatures Close to the Critical Temperature for Amorphization

Y Zhang,<sup>(a)</sup> C Wang,<sup>(a)</sup> MH Engelhard,<sup>(a)</sup> and WJ Weber<sup>(b)</sup>

(a) W.R. Wiley Environmental Molecular Sciences Laboratory, Richland, Washington

(b) Pacific Northwest National Laboratory, Richland, Washington

*Perovskites are the most abundant mineral on earth with a general formula of ABO<sub>3</sub>. Strontium titanate (SrTiO<sub>3</sub>) is a prominent representative of the group that is of technological interest in microelectronics and optoelectronic industries, as well as a potential material for immobilization of nuclear waste.*

Irradiation with energetic ions can be used to modify the surface and near-surface properties, inevitably produces defects and lattice disorder, and leads to amorphization. Previous irradiation studies (Zhang et al. 2005; White et al. 1988; Weber et al. 2000; Meldrum et al. 2002) indicate that SrTiO<sub>3</sub> undergoes an irradiation-induced crystalline to amorphous phase transition. The mechanism for irradiation-induced amorphization close to the critical temperature is, however, not well documented. To promote a better understanding of damage evolution, damage annihilation, and amorphization processes, this paper quantitatively characterizes damage accumulation on both the Sr and Ti sublattices as a function of dose under Au irradiation at temperatures close to the critical temperature for amorphization.

Ion irradiation, subsequent investigation of damage accumulation by Rutherford backscattering spectrometry (RBS), and cross-sectional transmission electron microscopy (TEM) in the SrTiO<sub>3</sub> single crystals were carried out using EMSL research facilities.

For irradiation at 360 K, which is just below the critical temperature (~370 K) for amorphization in the bulk, the depth profiles to various ion fluences are shown in Figure 1. The disorder on both the Sr and Ti sublattices increases with ion fluence. A fully amorphous layer is formed around 60 nm, following 1.2×10<sup>14</sup> cm<sup>-2</sup> irradiation at 360 K.

The damage evolution at 400 K, which is above the critical temperature for bulk amorphization in SrTiO<sub>3</sub>, is unusual as shown in Figure 2. For low ion fluences up to 1.5×10<sup>14</sup> cm<sup>-2</sup>, the relative disorder increases with increasing dose over the entire irradiation range, as expected. With further irradiation, the damage peak increases in width, but decreases in height. The damage saturates at a disorder level of ~0.75 under irradiation of 2.8×10<sup>14</sup> cm<sup>-2</sup>. For high ion fluence, the maximum damage appears at a deeper depth, where the damage accumulation stage and extended defect stage are delayed because of the nature of ion implantation. In addition, the saturation disorder level at 60 nm decreases. Under higher ion fluence irradiation, the supersaturation of point defects can cause agglomeration and formation of stable planar defects and dislocations (extended defect stage). The nucleation and growth of more complex defects, which act as sinks for point defects, effectively reduce the disorder accumulation rate. As the disorder level decreases at ~60 nm, the local dynamic annealing changes due to extend defect growth acting as a sink for point defects, and a new equilibrium state at lower disorder may eventually be reached. The unusual damage accumulation behavior is attributed to the formation and growth of stable extended defects.

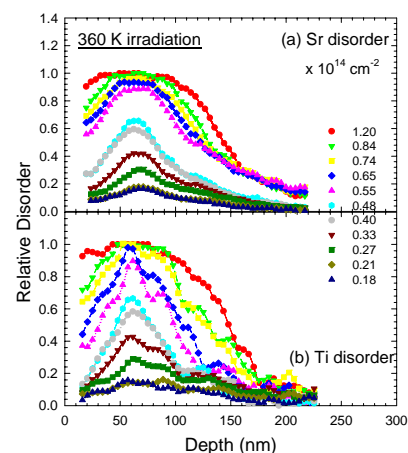


**Figure 1.** Disorder profiles on (a) Sr and (b) Ti sublattices under 1.0 MeV Au<sup>+</sup> irradiation at 360 K. The lines are smooth curve fits to the data to guide the eye.

Ion beam induced epitaxial crystallization (IBIEC) has attracted much attention over a few decades. The mechanisms of electronic and nuclear energy losses in IBIEC that are controlling the regrowth processes are not yet clear. In this study, electron beam (e-beam)-enhanced recrystallization is clearly observed before and after the electron-beam irradiation, as shown in Figure 3. This recrystallization may be attributed to localized electronic excitations that promote the rearrangement of interfacial atoms. It is worth pointing out that the e-beam flux during the TEM observation is on the order of  $10^{20}$   $\text{cm}^{-2}\text{s}^{-1}$ , which is eight orders of magnitude higher than the ion flux during the ion irradiation. Based on previous a recrystallization study on e-beam flux, the ion-induced dynamic recovery due to inelastic scattering processes in the current ion-irradiation study is negligible.

Under current irradiation conditions, nuclear stopping is a few times higher than electronic stopping over the whole irradiation region. During ion bombardment, the nuclear energy losses of the Au ions can efficiently transfer energy to a large number of target atoms in both the crystalline and damaged regions. The deposited energy can create defects, and stimulate defect migration and atomic rearrangement. At lower doses (i.e., the damage accumulation stage), the energy from Au ions is mainly transferred to atoms in the ordered crystalline structure; therefore, the fraction of damaged material increases with dose. As the irradiation dose increases (evolution stage), the probability for energy transfer from the Au ions to already disordered atoms increases, and the dynamic annealing of disordered atoms becomes more probable. When the effect of dynamic annealing is high enough to balance the ion-induced disordering, a saturation level is reached.

In this research, damage accumulation on both the Sr and Ti sublattices in strontium titanate ( $\text{SrTiO}_3$ ) has been investigated under 1.0 MeV  $\text{Au}^+$  irradiation at 360 and 400 K, close to the critical temperature for amorphization ( $\sim 370$  K). Under irradiation at 360 K, the relative disorder on both sublattices follows a nonlinear dependence on ion dose. Amorphization starts from the damage peak region (at a depth of 60 nm) and grows toward the surface and into the bulk. At 400 K, evolution of point defects to extended defects occurs as ion fluence increases. The disorder initially peaks at a depth of 60 nm, saturates at disorder level of  $\sim 0.75$ , and then decreases with further irradiation. At an ion fluence of  $6.0 \times 10^{15}$   $\text{cm}^{-2}$ , an amorphous layer of  $\sim 10$  nm thickness is formed at the sample surface.

### Citations

Meldrum A, LA Boatner, WJ Weber, and RC Ewing. 2002. "Amorphization and Recrystallization of the  $\text{ABO}_3$  Oxides." *Journal of Nuclear Materials* 300(2-3):242-254.

Weber WJ, W Jiang, S Thevuthasan, RE Williford, A Meldrum, and LA Boatner. 2000. *Defects and Surface-Induced Effects in Advanced Perovskites*. G. Borstel (ed.), p. 317, Kluwer Academic Publishers, The Netherlands.

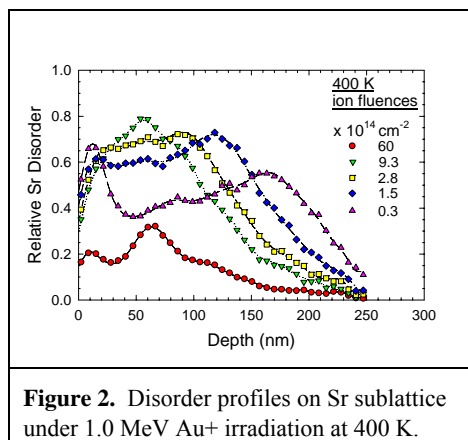


**Figure 2.** Disorder profiles on Sr sublattice under 1.0 MeV  $\text{Au}^+$  irradiation at 400 K.

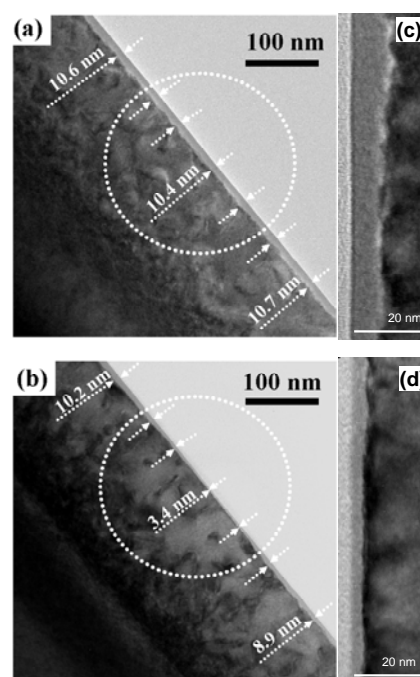


**Figure 3.** TEM images of a) the amorphous layer of  $\sim 10$  nm as indicated by the arrows. The dashed circle marks the electron irradiation area; b) the crystallization of amorphous layer following the e-beam irradiation; c) higher magnification image of the amorphous layer; and d) higher magnification image after the e-beam irradiation of the same region as shown in c).

White CW, LA Boatner, PS Sklad, CJ McHargue, J Rankin, GC Farlow, and MJ Aziz. 1988. "Ion Implantation and Annealing of Crystalline Oxides and Ceramic Materials." *Nuclear Instrumentation Methods Physics Research B* 32(1-4):11-22.

Zhang Y, J Lian, CM Wang, W Jiang, RC Ewing, and WJ Weber. 2005. "Ion-induced Damage Accumulation and Electron-beam-enhanced Recrystallization in SrTiO<sub>3</sub>." *Physical Review B* 72(9):094112-1-8.

## Crosslinked Enzyme Aggregates in Hierarchically Ordered Mesoporous Silica: A Simple and Effective Method for Enzyme Stabilization

MI Kim,<sup>(a)</sup> J Kim,<sup>(b)</sup> J Lee,<sup>(c)</sup> H Jia,<sup>(d)</sup> HB Na,<sup>(c)</sup> JK Youn,<sup>(a)</sup> JH Kwak,<sup>(b)</sup> A Dohnalkova,<sup>(e)</sup> JW Grate,<sup>(b)</sup> P Wang,<sup>(d)</sup> T Hyeon,<sup>(c)</sup> HG Park,<sup>(a)</sup> and HN Chang<sup>(a)</sup>

(a) Korea Advanced Institute of Science and Technology, Republic of Korea

(b) Pacific Northwest National Laboratory, Richland, Washington

(c) Seoul National University, Seoul, Republic of Korea

(d) University of Akron, Akron, Ohio

(e) W.R. Wiley Environmental Molecular Sciences Laboratory, Richland, Washington

*α*-Chymotrypsin (CT) and lipase (LP) were immobilized in hierarchically-ordered mesocellular mesoporous silica (HMMS) in a simple but effective way for the enzyme stabilization, which was achieved by the enzyme adsorption followed by glutaraldehyde (GA) crosslinking. This resulted in the formation of nanometer scale crosslinked enzyme aggregates (CLEAs) entrapped in the mesocellular pores of HMMS (37 nm), which did not leach out of HMMS through narrow mesoporous channels (13 nm). CLEA of *α*-chymotrypsin (CLEA-CT) in HMMS showed a high enzyme loading capacity and significantly increased enzyme stability. No activity decrease of CLEA-CT was observed for two weeks under even rigorously shaking condition, while adsorbed CT in HMMS and free CT showed a rapid inactivation because of the enzyme leaching and presumably autolysis, respectively. With the CLEA-CT in HMMS, however, there was no tryptic digestion observed, suggesting that the CLEA-CT is not susceptible to autolysis. Moreover, CLEA of lipase (CLEA-LP) in HMMS retained 30 percent specific activity of free lipase with greatly enhanced stability. This work demonstrates that HMMS can be efficiently employed as host materials for enzyme immobilization leading to highly enhanced stability of the immobilized enzymes with high enzyme loading and activity.

The preparation scheme of CLEAs in HMMS consists of two simple steps as depicted in Figure 1. The first step is to adsorb enzymes in HMMS, and the second step is to crosslink the adsorbed enzymes via glutaraldehyde treatment, resulting in nanometer-scale crosslinked enzyme aggregates (CLEAs) in the mesopores of HMMS. The structural properties of the employed HMMS are shown in Figure 1. A SEM image of the HMMS indicates that the component size of HMMS ranges from 200 to 500 nm. TEM image of the HMMS (Figure 2) shows the co-existence of large mesocellular pores (37 nm) and small mesoporous channels (13 nm). The channels are large enough for the enzymes to pass through without considerable diffusion limitation and the mesocellular pores can accommodate CLEAs.

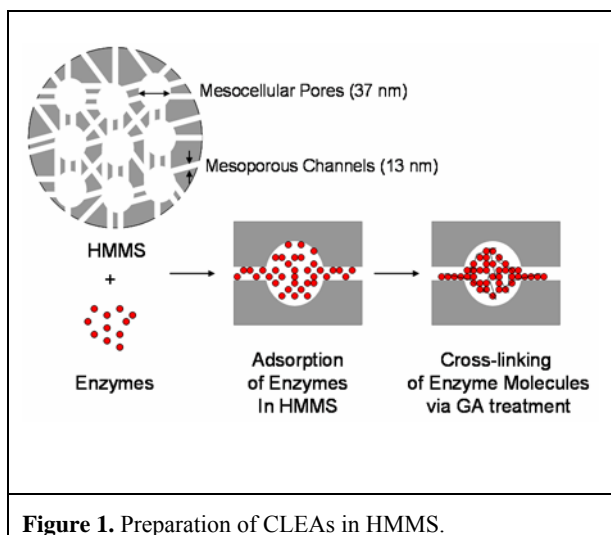
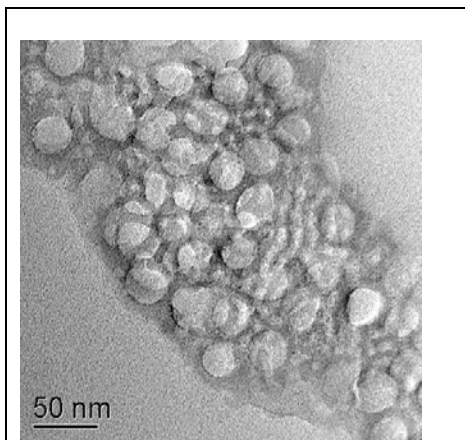


Figure 1. Preparation of CLEAs in HMMS.

We have demonstrated that the CLEAs entrapped in the mesocellular pores (37 nm) do not leach out through the mesoporous channels (13 nm) like in a ship-in-a-

bottle approach, leading to high-enzyme loading with concomitant improved stabilization of enzyme activity. The detailed mechanism of the ship-in-a-bottle approach has been elucidated in this paper.



**Figure 2.** TEM image of HMMS. Co-existence of large mesocellular pores and small mesoporous channels can be shown.

## Cycloaddition Functionalizations Preserve or Control Carbon Nanotube Conductance

YS Lee<sup>(a)</sup> and N Marzari<sup>(a)</sup>

(a) *Massachusetts Institute of Technology, Cambridge, Massachusetts*

*Carbon nanotubes continue to show promise for new materials with unique properties. By adding the right small molecules to a carbon nanotube, the ability to conduct electrons is modified. This could lead to a method of controlling a carbon nanotube's electrical properties.*

An extensive theoretical study on the energetics and quantum conductance of armchair carbon nanotubes functionalized with carbenes or nitrenes was performed (Figure 1). The groups are attached to neighboring carbon atoms forming a three-membered ring. The diameter of the tubes, relative angle of the sidewall carbon-carbon bond, and the chemical nature of the groups, determine the stability of the bond between the two sidewall carbons. This is radically at variance with the damage permanently induced by other common ligands, where a single covalent bond is formed with a sidewall carbon. Chirality, curvature, and chemistry determine bond cleaving, and in turn the electrical transport properties of a functionalized tube. A well-defined range of diameters can be found for which certain addends exhibit a

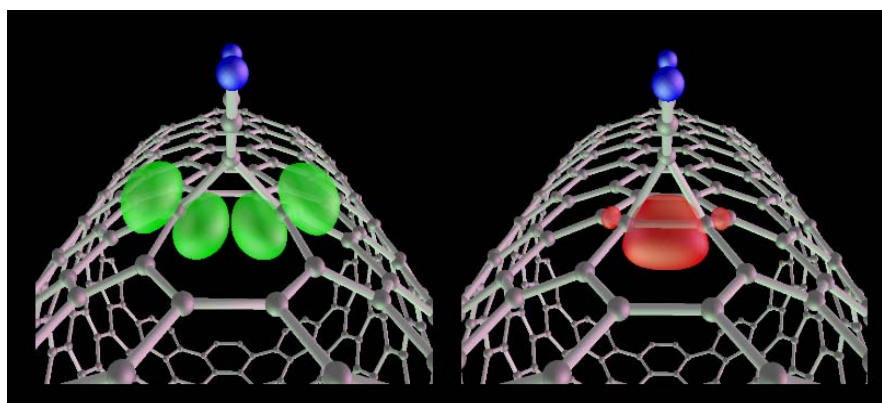


**Figure 1.** Two tautomeric states show different conductance states suggesting a novel conductance-control mechanism. Orbital rehybridization through bond breaking and forming can be applied to both semiconducting and metallic nanotubes.

bistable state, where the opening or closing of the sidewall bond, accompanied by a switch in the conductance, could be directed with chemical, optical, or thermal means.

Two conclusions can be drawn. First, even with a large number of functional groups, the conductance remains high when cycloadditions break the sidewall bond. Second, a subclass of substituents can be found (e.g.,  $C(CN)_2$ ) that stabilizes two tautomeric forms on the same tube, separately displaying high and low conductance.

## Lattice Strain Effects on Carbon Monoxide Oxidation on a Platinum(111) Surface

L Grabow,<sup>(a)</sup> Y Xu,<sup>(b)</sup> and M Mavrikakis<sup>(a)</sup>

(a) University of Wisconsin at Madison, Madison, Wisconsin

(b) Oak Ridge National Laboratory, Oak Ridge, Tennessee

*Carbon monoxide is very toxic and odorless. Understanding how carbon monoxide is oxidized on a catalytic surface by oxygen can lead to better, more efficient ways to remove this molecule from internal combustion engine and other sources.*

Strain can significantly affect binding energies of adsorbed species and activation energy barriers of surface reactions. Density functional theory was used in combination with microkinetic modeling to establish the foundations of the qualitative analysis presented by Cirak et al. 2003 and provide insights for a deeper understanding of the effect of surface strain on catalytic reactions in general. Accordingly, the first-ever quantitative analysis of chemo-mechanical coupling as it manifests itself on surface reactivity was carried out. The results of our first principles calculations are summarized in a potential energy surface (PES) given in Figure 1. The rate limiting step can be changed by manipulating the strain. When the platinum surface is compressed the barrier is higher, but when the platinum surface is stretched the barrier is lower than a relaxed platinum surface.

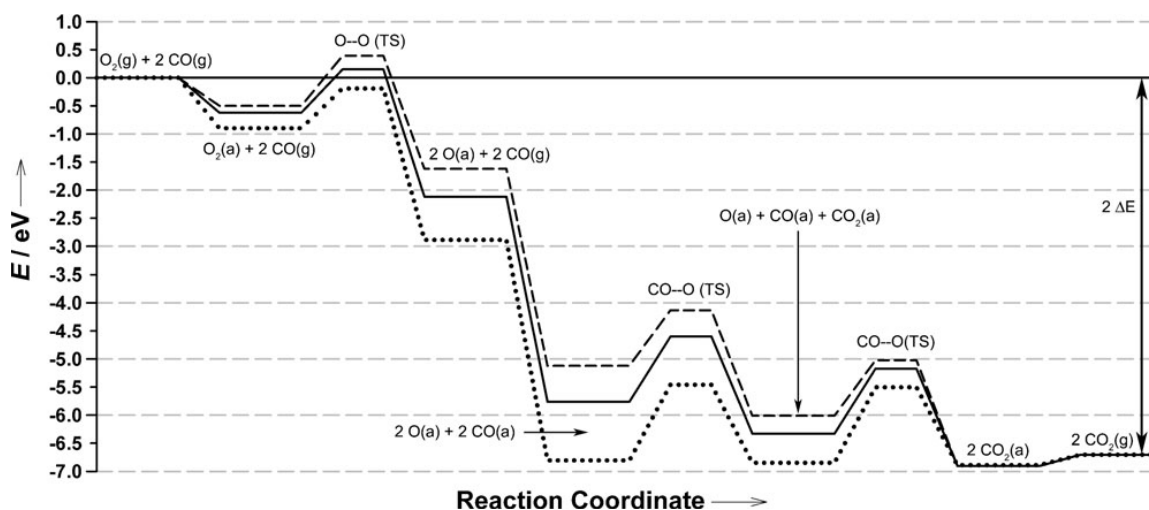


**Figure 1.** Overall PES for carbon monoxide oxidation on Pt(111) for equilibrium lattice constant (—), 2%-compressed (---), and 4%-stretched (···). ( $2*\Delta E$ ) represents the heat of the overall reaction:  $O_2(g) + 2CO(g) \rightarrow 2CO_2(g)$ , where (g) indicates gas phase species. In the graph, TS indicates the transition state of the respective elementary step.

## Citation

Cirak F, JE Cisternas, AM Cuitino, G Ertl, P Holmes, IG Kevrekidis, M Ortiz, HH Rotermund, M Schunack, and J Wolff. 2003. “Oscillatory Thermomechanical Instability of an Ultrathin Catalyst.” *Science* 300(5627):1932-1936.

## Scientific Grand Challenge Highlights

In December 2006, S Bose successfully defended his thesis entitled “Bioreduction of Hematite Nanoparticles by *Shewanella oneidensis* MR-1” and earned a Doctorate of Philosophy in Geosciences from Virginia Polytechnic Institute and State University (Virginia Tech). His research was conducted at EMSL as part of the Biogeochemistry Scientific Grand Challenge and in collaboration with EMSL scientists BH Lower, A Dohnalkova, and D McCready. His work resulted in two publications, one published in the *Journal of the American Chemical Society* and one that will be submitted to *Geochimica et Cosmochimica Acta*. Bose is beginning a postdoctoral fellowship at the University of California at Berkeley in the laboratory of Professor J Coates where he will focus his research on the development of biofuel cells.

## Professional/Community Service

**EMSL Hosts NWChem Meeting.** The “NWChem Meeting on Science Driven Petascale Computing and Capability Development at EMSL,” was held on January 25 and 26, 2007, at EMSL. With 65 people in attendance, leading scientists from universities and national laboratories presented their vision on future scientific challenges and the role that petascale computing can play in answering those scientific problems. Topics covered included the status and future direction of NWChem, going open-source with NWChem, how we can contribute to the growth of NWChem related to its scientific capability and computational performance by 2022, new computational chemistry methodologies, and computer science needs to enable parallel implementation on petascale. The information generated by the participants’ discussions will be rolled into a meeting report and a subsequent strategic plan for further development of NWChem.

**Scientific Facility Lead Featured in “Mid-Columbian Magazine.”** R Gephart, Scientific Facility Lead for the Chemistry and Physics of Complex Systems Facility, was featured in the January 2007 issue of the “Mid-Columbian” for his volunteer efforts with the Tri-City Astronomy Club. On November 8, 2006, Gephart was actively involved in furthering the astronomical education of local students who visited the Moore Observatory at Columbia Basin College campus in Pasco for a glimpse of a rare event: the transit of the planet Mercury across the Sun.

## Major Facility Upgrades

**Ribbon Cutting Celebrates First Permanent Expansion of EMSL.** An informal ribbon cutting of the new supercomputing raised floor in the Molecular Science Computing Facility was held on January 10, 2007, to give staff and users a sense of celebration as well as knowledge that the facility is growing and will continue to grow during the next decade. The new ~ 4000-square-foot raised floor constitutes the first-ever permanent expansion of EMSL. One hundred and seventy-five people attended the ceremony.

Cabling and cooling capabilities will be located under the floor, and the room itself will provide space for expansion of the MSCF’s data archive capabilities as well as house at least a portion of the next-generation supercomputer, which is scheduled for operation in 2008.

The Request for Proposal (RFP) call was released on January 19, 2007 for the vendor review and contract award for the HPCS-3 SuperComputer. The deadline for responses is March 2, 2007. After the Source

Selection Panel (SSP) reviews the responses to the RFP, they will vote for the vendor who provides the best computer resources for the least cost. This will also be based on the amount of “value-adds” the vendor is able to provide within the same cost estimate.

**SPLAT II: Second-Generation Single Particle Laser Ablation Time-of-Flight Mass Spectrometer** is a second-generation, single-particle, laser-ablation, time-of-flight mass spectrometer (Figure 1). It is a unique, high-precision instrument that allows users to study the fundamental processes that govern the chemistry and physics of particles on the nano- and micro-scales. Applications for the new instrument include, but are not limited to, climate, air pollution, human health, bioterrorism, and emerging nanotechnologies.

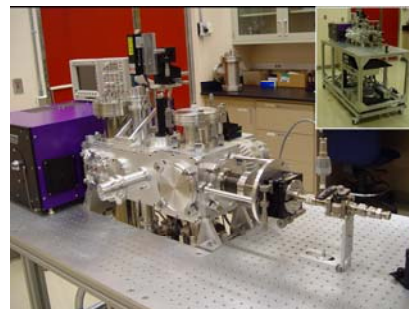


**Figure 1.** SPLAT II was constructed using capability funds from both EMSL and Basic Energy Sciences.

Portability is a hallmark of SPLAT II. It is the first field-deployable instrument that provides in real time, the size, density, shape, fractal dimension, and composition of individual particles down to 50 nm in diameter. It is the first field instrument operated in an infrared-ultraviolet (IR-UV) mode, thereby enabling the collection of reproducible and quantitative particle mass spectra.

SPLAT II uses an extremely efficient aerodynamic lens inlet to produce a narrow (250  $\mu\text{m}$ ) low divergent particle beam. Two stages of differential pumping separate particles and gas. Two stages of optical detection use light scattering to detect each particle twice and to measure its velocity, from which the aerodynamic diameter particle of the can be determined. Pulsed, synchronized IR evaporation followed by UV ionization of semi-volatile

fractions and ablation of non-volatile fractions creates ions. From these ions, time-of-flight mass spectra are generated for compositional analysis (Figure 2).

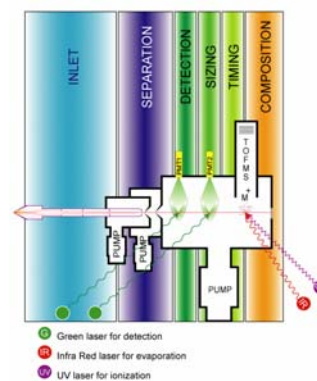


**Figure 2.** Extremely efficient aerodynamics lens inlet.

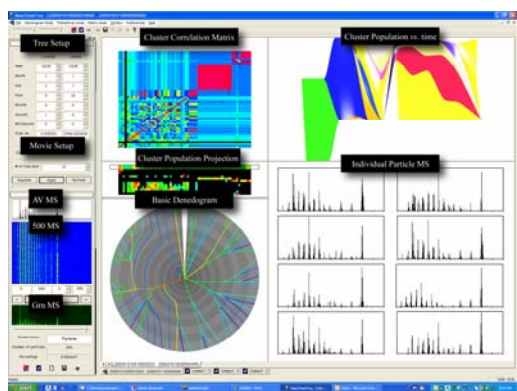


**Figure 3.** SpectraMiner presents a multitude of views to the scientist.

SpectraMiner is a dedicated data mining and visualization software specifically designed to explore single-particle mass spectra (Figure 3). It helps researchers make use of the vast amounts of detailed data generated by SPLAT II. SpectraMiner puts the scientist at the center of the data mining process, providing intuitive controls that connect the particle data with any other relevant events pushing the knowledge beyond simple statistical analysis.

**The X-band electron paramagnetic resonance spectrometer** in the Environmental Spectroscopy and Biogeochemistry Facility was returned to service after upgrading the microwave source and the source control. EMSL user S Miller used the upgraded system to analyze borosilicate glass samples for radiation-generated free radicals and reported excellent results.

## Visitors and Users

During this reporting period, a total of 340 users benefited from EMSL capabilities and expertise. This total included 168 onsite users and 172 remote users.

## Publications

Antony J, Y Qiang, M Faheem, D Meyer, DE McCready, and MH Engelhard. 2007. “Ferromagnetic Semiconductor Nanoclusters: Co-doped Cu<sub>2</sub>O.” *Applied Physics Letters* 90(1): Art. No. 013106.

Averkiev BB, AI Boldyrev, X Li, and LS Wang. 2007. “Probing the Structure and Bonding in Al<sub>6</sub>N and Al<sub>6</sub>N by Photoelectron Spectroscopy and *Ab Initio* Calculations.” *Journal of Physical Chemistry A* 111(1):34-41.

Barcaro G, A Fortunelli, G Rossi, F Nita, and R Ferrando. 2006. “Electronic and Structural Shell Closure in AgCu and AuCu Nanoclusters.” *Journal of Physical Chemistry B* 110(43):23197-23203.

Bae I, Y Zhang, WJ Weber, M Higuchi, and L Giannuzzi. 2007. “Electron-Beam Induced Recrystallization in Amorphous Apatite.” *Applied Physics Letters* 90(2): Art. No. 021912.

Berryman OB, V Bryantsev, DP Stay, DW Johnson, and BP Hay. 2007. “Structural Criteria for the Design of Anion Receptors: The Interaction of Halides with Electron-Deficient Arenes.” *Journal of the American Chemical Society* 129(1):48-58.

Bertino MF, Z Sun, R Zhang, and LS Wang. 2006. “Facile Syntheses of Monodisperse Ultrasmall Au Clusters.” *Journal of Physical Chemistry B* 110(43):21416-21418.

Cai M, SC Langford, MJ Wu, WM Huang, G Xiong, TC Droubay, AG Joly, K Beck, WP Hess, and JT Dickinson. 2007. “Study of Martensitic Phase Transformation in a NiTiCu Thin-Film Shape-Memory Alloy Using Photoelectron Emission Microscopy.” *Advanced Functional Materials* 17(1):161-167.

Cheng C, JC Lehmann, JE Thies, SD Burton, and MH Engelhard. 2006. “Oxidation of Black Carbon by Biotic and Abiotic Processes.” *Organic Geochemistry* 37(11):1477-1488.

Crocombette J, G Dumazer, NQ Hoang, F Gao, and WJ Weber. 2007. “Molecular Dynamics Modeling of the Thermal Conductivity of Irradiated SiC as a Function of Cascade Overlap.” *Journal of Applied Physics* 101(2): Art. No. 023527.

Crosby L and HA Kurtz. 2006. “Application of Electronic Structure and Transition State Theory: Reaction of Hydrogen with Silicon Radicals.” *International Journal of Quantum Chemistry* 106(15):3149-3159.

Dantas G, AL Watters, B Lunde, Z Eletr, NG Isern, T Roseman, J Lipfert, S Doniach, M Tompa, B Kuhlman, BL Stoddard, G Varani, and D Baker. 2006. “Mistranslation of a Computationally Designed Protein Yields an Exceptionally Stable Homodimer: Implications for Protein Engineering and Evolution.” *Journal of Molecular Biology* 362(5):1004-1024.

Del Negro AS, CJ Seliskar, WR Heineman, SE Hightower, SA Bryan, and BP Sullivan. 2006. “Highly Oxidizing Excited States of Re and Tc Complexes.” *Journal of the American Chemical Society* 128(51):16494-16495.

Farnan I, HM Cho, and WJ Weber. 2007. “Quantification of Actinide  $\alpha$ -Radiation Damage in Minerals and Ceramics.” *Nature* 445(7124):190-193.

Forquer IP, R Covian, MK Bowman, B Trumppower, and DM Kramer. 2006. “Similar Transition States Mediate the Q-cycle and Superoxide Production by the Cytochrome bc<sub>1</sub> Complex.” *Journal of Biological Chemistry* 281(50):38459-38465.

Gun'ko VM, EF Voronin, LV Nosach, EM Pakhlov, O Voronina, NV Guzenko, O Kazakova, R Lebeda, and J Skubiszewska-Zieba. 2006. “Nanocomposites with Fumed Silica/Poly(Vinyl Pyrrolidone) Prepared at a Low Content of Solvents.” *Applied Surface Science* 253(5):2801-2811.

Gutowski KE, VA Cocalia, ST Griffin, NJ Bridges, DA Dixon, and RD Rogers. 2007. “Interactions of 1-Methylimidazole with UO<sub>2</sub>(CH<sub>3</sub>CO<sub>2</sub>)<sub>2</sub> and UO<sub>2</sub>(NO<sub>3</sub>)<sub>2</sub>: Structural, Spectroscopic, and Theoretical Evidence for Imidazole Binding to the Uranyl Ion.” *Journal of the American Chemical Society* 129(3):526-536.

Hixson KK, JN Adkins, SE Baker, RJ Moore, BA Chromy, RD Smith, SL McCutchen-Maloney, and MS Lipton. 2006. “Biomarker Candidate Identification in *Yersinia pestis* Using Organism-Wide Semiquantitative Proteomics.” *Journal of Proteome Research* 5(11):3008-3017.

Jastrow JD, JE Amonette, and VL Bailey. 2007. “Mechanisms Controlling Soil Carbon Turnover and Their Potential Application for Enhancing Carbon Sequestration.” *Climatic Change* 80(1-2):5-23.

Jiang W, Y Zhang, MH Engelhard, WJ Weber, GJ Exarhos, J Lian, and RC Ewing. 2007. “Behavior of Si and C Atoms in Ion Amorphized SiC.” *Journal of Applied Physics* 101(2): Art. No. 023524.

Jiang W, Y Zhang, V Shutthanandan, S Thevuthasan, and WJ Weber. 2006. “Temperature Response of <sup>13</sup>C Atoms in Amorphized 6H-SiC.” *Applied Physics Letters* 89(26): Art. No. 261902.

Johnson BR, NL Canfield, DN Tran, RA Dagle, XS Li, JD Holladay, and Y Wang. 2007. “Engineered SMR Catalysts Based on Hydrothermally Stable, Porous, Ceramic Supports for Microchannel Reactors.” *Catalysis Today* 120(1):54-62.

Kelly RT, JS Page, Q Luo, RJ Moore, DJ Orton, K Tang, and RD Smith. 2006. “Chemically Etched Open Tubular and Monolithic Emitters for Nanoelectrospray Ionization Mass Spectrometry.” *Analytical Chemistry* 78(22):7796-7801.

Kowalski K and M Valiev. 2006. “Asymptotic Extrapolation Scheme for Large-Scale Calculations with Hybrid Coupled Cluster and Molecular Dynamics Simulations.” *Journal of Physical Chemistry A* 110(48):13106-13111.

Labello NP, AM Ferreira, and HA Kurtz. 2006. “Utilizing Relativistic Effective Core Potentials for Accurate Calculations of Molecular Polarizabilities on Transition Metal Compounds.” *Journal of Physical Chemistry A* 110(50):13507-13513.

Lepetit C, H Chermette, M Gicquel, J Heully, and R Chauvin. 2007. “Description of Carbo-oxocarbons and Assessment of Exchange-Correlation Functionals for the DFT Description of Carbo-mers.” *Journal of Physical Chemistry A* 111(1):136-149.

Leung H and F Naumkin. 2006. “Induced Super-halogen Behavior of Metal Moieties in Halogen-Doped Clusters: Li<sub>n</sub>I<sup>+</sup> and Al<sub>n</sub>I<sup>+</sup>, n = 13, 1, 2, 3.” *Journal of Physical Chemistry A* 110(50):13514-13520.

Liu C, JM Zachara, W Yantasee, PD Majors, and JP McKinley. 2006. “Microscopic Reactive Diffusion of Uranium in the Contaminated Sediments at Hanford, United States.” *Water Resources Research* 42: Art.

No.W12420.

Liu T, W Qian, HM Mottaz, MA Gritsenko, AD Norbeck, RJ Moore, SO Purvine, DG Camp II, and RD Smith. 2006. "Evaluation of Multiprotein Immunoaffinity Subtraction for Plasma Proteomics and Candidate Biomarker Discovery Using Mass Spectrometry." *Molecular & Cellular Proteomics (MCP)* 5(11):2167-2174.

Lyon JT and L Andrews. 2007. "An Infrared Spectroscopic and Theoretical Study of Group 4 Transition Metal  $\text{CH}_2=\text{MCl}_2$  and  $\text{HC} \div \text{MCl}_3$  Complexes." *Organometallics* 26(2):332-339.

Mazurkiewicz K, R Bachorz, MS Gutowski, and J Rak. 2006. "On the Unusual Stability of Valence Anions of Thymine Based on Very Rare Tautomers: A Computational Study." *Journal of Physical Chemistry B* 110(48):24696-24707.

Mulas G, G Mallocci, C Joblin, and D Toubanc. 2006. "A General Model for the Identification of Specific PAHs in the Far-IR." *Astronomy & Astrophysics: A European Journal* 460(1):93-104.

Peterson KA, BC Shepler, D Figgen, and H Stoll. 2006. "On the Spectroscopic and Thermochemical Properties of ClO, BrO, IO, and Their Anions." *Journal of Physical Chemistry A* 110(51):13877-13883.

Qafoku O and AR Felmy. 2007. "Development of Accurate Chemical Equilibrium Models for Oxalate Species to High Ionic Strength in the System: Na-Ba-Ca-Mn-Sr-Cl-NO<sub>3</sub>-PO<sub>4</sub>-SO<sub>4</sub>-H<sub>2</sub>O at 25°C." *Journal of Solution Chemistry* 36(1):81-95.

Resch W, Hixson KK, Moore RJ, Lipton MS, and Moss B. 2007. "Protein Composition of the Vaccinia Virus Mature Virion." *Virology* 358(1):233-47.

Sebetci A. 2006. "A Density Functional Study of Bare and Hydrogenated Platinum Clusters." *Chemical Physics* 331(1):9-18.

Shvartsburg AA, T Bryskiewicz, R Purves, K Tang, R Guevremont, and RD Smith. 2006. "Field Asymmetric Waveform Ion Mobility Spectrometry Studies of Proteins: Dipole Alignment in Ion Mobility Spectrometry?" *Journal of Physical Chemistry B* 110(43):21966-21980.

Teeguarden JG, PM Hinderliter, G Orr, BD Thrall, and JG Pounds. 2007. "Particokinetics *In Vitro*: Dosimetry Consideration for *In Vitro* Nanoparticle Toxicity Assessments." *Toxicological Sciences* 95(2):300-312.

Thornton EC, L Zhong, and M Ostrom. 2006. "Development of a Field Design for *In Situ* Gaseous Treatment of Sediment Based on Laboratory Column Test Data." *Journal of Environmental Engineering* 132(12):1626-1632.

Umar AN, TM Luider, JA Foekens, and L Pasa-Tolic. 2007. "Nano-LC-FT-ICR MS Improves Proteome Coverage Attainable for ~3000 Laser-microdissected Breast Carcinoma Cells." *Proteomics* 7(2):323-329.

Valiev M and K Kowalski. 2006. "Hybrid Coupled Cluster and Molecular Dynamics Approach: Application to the Excitation Spectrum of Cytosine in the Native DNA Environment." *Journal of Chemical Physics* 125(21): Art. No. 211101.

Wang Z, X Zu, F Gao, and WJ Weber. 2006. "Atomistic Simulation of Brittle to Ductile Transition in GaN Nanotubes." *Applied Physics Letters* 89(24): Art. No. 243123.

Wind RA, and J Hu. 2006. "*In Vivo* and *Ex Vivo* High-Resolution <sup>1</sup>H NMR in Biological Systems Using Low-Speed Magic Angle Spinning." *Progress in Nuclear Magnetic Resonance Spectroscopy* 49(3-4):207-259.

Witek HA, S Irle, G Zheng, WA De Jong, and K Morokuma. 2006. “Modeling Carbon Nanostructures with the Self-Consistent Charge Density-Functional Tight-Binding Method: Vibrational and Electronic Spectra of C<sub>28</sub>, C<sub>60</sub>, and C<sub>70</sub>.” *Journal of Chemical Physics* 125(21): Art. No. 214706.

Yantasee W, C Timchalk, and Y Lin. 2007. “Microanalyzer for Biomonitoring of Lead (Pb) in Blood and Urine.” *Analytical and Bioanalytical Chemistry* 387(1):335-341.

Zelenyuk AN, DG Imre, Y Cai, K Mueller, Y Han, and P Imrich. 2006. “SpectraMiner, An Interactive Data Mining and Visualization Software for Single Particle Mass Spectroscopy: A Laboratory Test Case.” *International Journal of Mass Spectrometry* 258(1-3):58-73.

Zhao H, J Kwak, Y Wang, JA Franz, JM White, and JE Holladay. 2007. “Interactions between Cellulose and N-Methylmorpholine-N-Oxide.” *Carbohydrate Polymers* 67(1):97-103.

## Presentations

- Annual Workshop and Business Meeting of the AirUCI Environmental Molecular Science Institute, December 2006, Christchurch, New Zealand.
- American Geophysical Union Fall Meeting, December 2006, San Francisco, California.
- IWOX 5<sup>th</sup> International Workshop on Oxide Surfaces, January 2007, Lake Tahoe, California.
- Mebatoblic Markers Conference, December 5, 2006, Orlando, Florida.
- MSCF Debugging Workshop, December 19, 2006, Richland, Washington.
- NWChem Meeting: Science-Driven Petascale Computing and Capability Development at the EMSL, January 25, 2007, Richland, Washington.
- Scientific Computing Presents, “WebCast: Are They Ready for Your HPC Demands?” December, 20, 2006, Chicago, Illinois.
- Washington State University Chemistry Department Seminar Series, December 4, 2006, at Pullman, Washington.
- Work Based Learning Class, January 3, 2007, at Richland High School, Richland, Washington.